Stimulated orientational scattering and third-order nonlinear optical processes in nematic liquid crystals

P. Etchegoin* and R. T. Phillips
Cavendish Laboratory, University of Cambridge, Madingley Road, CB3 OHE, Cambridge, United Kingdom
(Received 3 July 1996)

We study two different effects intimately related to the existence of a third-order nonlinear optical susceptibility $\chi^{(3)}$ in a nematic liquid crystal. We first present data and calculations on stimulated orientational scattering and show that it can be accounted for by a four-wave mixing process in which noise is coherently amplified to the extent that it can deplete the input pump wave almost completely. On the other hand, we show the formal relation between four-wave mixing (as a laser-induced grating process) and the theory of photonic band structures, giving rise to a suitable formalism for the study of different experimental situations. It is suggested that the *photonic crystal* approach to four-wave mixing can be used to evaluate the diffraction efficiencies of the probe beam for different polarizations and scattering directions in a relatively easy manner. Finally, we predict by using this formalism the existence of *umklapp four-wave mixing* events in which the phase matching of the waves is achieved by a reciprocal lattice vector of the grating itself. [S1063-651X(96)02112-5]

PACS number(s): 61.30.Gd, 42.70.Df, 42.65.Hw, 42.65.Jx

I. INTRODUCTION AND OVERVIEW

The field of nonlinear optical properties of liquid crystals is in a relatively mature stage [1]. Liquid crystals are notorious for the large magnitude of their nonlinear optical susceptibilities. Typically, a nematic liquid crystal will have a third-order nonlinear optical susceptibility $\chi^{(3)}$ of the order of $\sim 10^{-22}$–10^{-23} Cm V^{-3}, which is about eight orders of magnitude larger than that of CS_2 [1]. These large optical susceptibilities allowed the observation of several nonlinear optical effects at relatively low powers by using constant wave (CW) lasers instead of the high-power pulsed lasers normally needed for semiconductors [1]. In this paper we deal with two CW-nonlinear optical effects related to the existence of a large $\chi^{(3)}$ in nematics. A brief description of the underlying concepts needed for the discussion and the general aims of the paper are given here in what follows.

The macroscopic order of a nematic liquid crystal at any point in space $\vec{r}$ is specified by the director $\vec{n}(\vec{r})$ [2]. Nematic liquid crystals are centrosymmetric in all their physical properties depending on $\vec{n}(\vec{r})$, i.e., although the individual molecules (or mixtures of molecules) may not have inversion symmetry, the nematic state is such that the macroscopic physical properties are not changed by the operation $\vec{n}(\vec{r}) \rightarrow -\vec{n}(\vec{r})$. The latter is one of the fundamental assumptions of the theory of the nematic state [2]. The centrosymmetric character infers from the point of view of the nonlinear optical properties that $\chi^{(2)}=0$, in other words, second harmonic generation, up- and down-conversions, parametric amplifications or oscillations, etc., are all forbidden in bulk nematics [3]. The lowest possible nonlinear optical susceptibility is therefore $\chi^{(3)}$, which is responsible for two- and four-wave mixings [1], self-focusing and self-phase modulations [4], stimulated Raman and Brillouin scattering [5], third harmonic generation [6], etc. The microscopic origin of $\chi^{(3)}$ in liquid crystals can vary according to the experimental circumstances but, essentially, it may come from either electronic transitions, molecular reorientations, density and temperature gratings, or combinations of them [7]. In the transparency region, which for most nematic liquid crystals extends through the visible range, all mechanisms are important under the appropriate circumstances, except the electronic contributions, which are small far from the lowest highest-occupied-molecular-orbital (HOMO) to lowest-unoccupied-molecular-orbital (LUMO) transition [1].

So far, we have established that the nematic state will have a large nonlinearity $\chi^{(3)} \neq 0$ and that different mechanisms can contribute to it. On the other hand, the *linear* optical properties are characterized by a birefringent medium. Nematics are naturally birefringent due to the fact that the refractive indices for polarization $\parallel$ or $\perp$ to $\vec{n}(\vec{r})$ $(n_{\parallel}, n_{\perp})$ are different, and large optical anisotropies in the visible $\Delta n = n_{\parallel} - n_{\perp} \sim 0.2$ are commonly found. A key feature of nematics is also the high efficiency with which they scatter light elastically [8,9] through fluctuations in the director. Elastic light scattering is in fact smaller in the isotropic phase of a liquid crystal (where the molecules are randomly oriented) than in the nematic state [1] and this is easily seen through a characteristic *dynamic laser speckle pattern* observed in lasers crossing a nematic cell. The drastic change in the elastic scattering cross section between the isotropic and the nematic state is, in fact, the reason for calling the nematic-to-isotropic phase transition temperature a *clearing point*.

We now have all the tools needed to introduce the origin of *stimulated orientational scattering* (SOS). Suppose we have the following situation: an optical plane wave is sent though a nematic so that its polarization is either perpendicular (ordinary, or *o* ray) or parallel (extraordinary,

*Permanent address: Centro Atómico Bariloche and Instituto Balseiro, Comisión Nacional de Energía Atómica and Universidad Nacional de Cuyo, 8400 San Carlos de Barlioche, Río Negro, Argentina.

or *e* ray) to the director $\vec{n}$. We know the medium has $\chi^{(3)} \neq 0$ but, as we shall show in Sec. II, unless additional waves are introduced, $\chi^{(3)}$ can only produce self-phase modulation of the wave (or transverse phase modulation if the beam is not a plane wave) but not change its polarization. On the other hand, we have a very large cross section for elastic scattering through fluctuations of the director which can produce waves of any polarization. In a linear medium this would simply result in loss and degradation of the polarization state of the input pump wave and the generation of scattered *noise* waves. In this particular case, however, both mechanism can cooperate to give rise to the appearance of a new phenomenon. A small portion of the input wave (say, *o* ray) scattered perpendicularly (*e* ray) can now couple through $\chi^{(3)}$ to the input wave again and actually grow coherently out of this interaction. Following the general principles of stimulated and spontaneous emission [10], the new wave may become stimulated if the pump power is high enough to overcome the inevitable losses. This is the underlying principle of SOS. Essentially, a cross-polarized wave with respect to the pump is monitored in transmission through a nematic liquid crystal and exponential growth is observed above a certain threshold. This *transfer* of energy between the two polarizations has its roots in the interplay between noise and nonlinearity. In a broader sense, SOS is not the only known case of cooperation between noise and nonlinearity. The most celebrated example of this kind is probably the phenomena of *stochastic resonances* [11] in which a signal buried in noise in a nonlinear system is amplified (and its signal-to-noise ratio improved) by actually *increasing* the noise amplitude; something completely contrary to the premises of linear systems.

The transient aspects of the orientational scattering have been studied by Zel'dovich *et al.* [12] using pulsed lasers. More recently, Khoo, Liang, and Li [13] correctly predicted with a coupled wave formalism the existence of SOS using low-power CW lasers and observed it experimentally in nematics, together with self-starting phase conjugation. In Sec. III we give a slightly different treatment of SOS. We show that SOS can be conceived as a degenerate four-wave mixing process coupling the *o* and *e* rays (with both $+\vec{k}$ and $-\vec{k}$) and we show that the stimulated wave not only grows exponentially above a certain threshold but also may display saturation effects by depleting the pump. We show data for the various polarizations and demonstrate the existence of saturation phenomena. The experiments (in particular, the saturation effects) are compared with the predictions of the four-wave mixing treatment.

Moreover, the second part of the paper (Sec. IV) presents an analogy which may prove useful in studying wave mixing phenomena in liquid crystals and beyond. In recent years, it has become increasingly apparent that the propagation of electromagnetic waves in periodic dielectric structures (PDS's) is not only very interesting but also displays new wave phenomena [14]. A great deal of work using different methods has been done to calculate the so-called *photonic band structures* of the electromagnetic waves in a periodic grating made of dielectrics. Likewise, the phenomenon of four-wave mixing can, in some cases, be regarded as diffraction of a probe beam produced by a laser-induced grating. The grating is created by two interfering pump beams normally of higher intensity than the probe. Therefore, an obvious question arises regarding the possible link between these two distinct problems. The formal connection between the four wave-mixing equations and the theory of photonic crystals is given in Sec. IV. It is shown how the link can be used backwards to predict, among other things, diffraction efficiencies of the four-wave mixing signals and the existence of umklapp processes. In the latter, the phase-matching condition of the four waves is achieved through a reciprocal lattice vector of the laser-induced grating itself.

In order to develop the above-mentioned effects further, a brief introduction to the nonlinear coupled Maxwell equations with $\chi^{(3)} \neq 0$, to uniformize the notation and facilitate the discussion, is unavoidable. This is done in Sec. II.

II. COUPLED MAXWELL EQUATIONS WITH $\chi^{(3)} \neq 0$

This section is a standard textbook example of coupled Maxwell equations in nonlinear optics. We therefore keep details to a bare minimum and refer the reader to some of the best known books in the field. We follow closely Refs. [1,16–18] in the presentation.

Consider a nonlinear optical material with $\chi^{(2)}=0$ and $\chi^{(3)} \neq 0$. Its polarization P will be given by

$$P = \epsilon_0 \chi E + 4\chi^{(3)} E^3 = \epsilon_0 \chi E + P_{nl}, \tag{1}$$

where E is the electric field of the light, χ the linear optical susceptibility, and ϵ_0 the permittivity of free space. We drop indices in the vectors and tensors to facilitate the notation. We also assume χ and $\chi^{(3)}$ to be dispersionless in the region of interest [19]. Maxwell equations for the electric field of the light become [16–18]

$$\nabla^2 E - \frac{n^2}{c^2}\frac{\partial^2 E}{\partial t^2} = \mu_0 \frac{\partial^2 P_{nl}}{\partial t^2}, \tag{2}$$

with $P_{nl}=4\chi^{(3)}E^3$, c the speed of light in a vacuum, μ_0 the permeability of free space, and $n^2=1+\chi$ the linear index of refraction. By assuming the field E to be a linear combination of four waves

$$E(t) = \sum_{q=1,\ldots 4} \mathrm{Re}[E_q e^{i\omega_q t}] \tag{3}$$

with $E_q = A_q \exp(-i\vec{k}_q \cdot \vec{r})$, and collecting terms of the same frequencies in (2), four Helmholtz equations are obtained of the form

$$\left(\nabla^2 + \frac{n^2\omega_q^2}{c^2}\right) E_q = \hat{S}_q + \left(\frac{\omega_q}{c}\right)^2 \Delta\chi_q E_q, \quad q=1,\ldots,4 \tag{4}$$

with $\hat{S}_1 = 6\mu_0\omega_1^2\chi^{(3)}E_3E_4E_2^*$, $\hat{S}_2 = 6\mu_0\omega_2^2\chi^{(3)}E_3E_4E_1^*$, $\hat{S}_3 = 6\mu_0\omega_3^2\chi^{(3)}E_1E_2E_4^*$, $\hat{S}_4 = 6\mu_0\omega_4^2\chi^{(3)}E_1E_2E_3^*$, and $\Delta\chi_q = (6\gamma/\epsilon_0)\chi^{(3)}(2I - I_q)$, where $I_q = |E_q|^2/2\gamma$, $(\gamma = \sqrt{\mu_0/\epsilon_0}/n)$ and $I = I_1 + I_2 + I_3 + I_4$ the total and individual intensities of the waves, respectively. The four-wave mixing process can be interpreted as a photon interaction given by the Feynmam diagram of Fig. 1, where energy and wave-vector conservation (phase matching) require

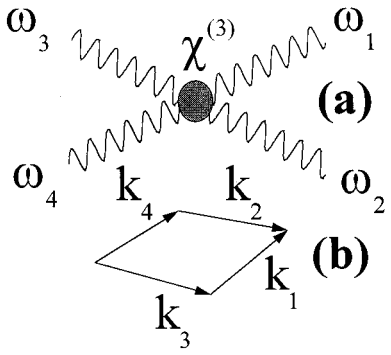

FIG. 1. Four-wave mixing process as a photon interaction. The mixing is governed by the coupled nonlinear equations (4) and the requirement of energy conservation and phase matching of the waves implies $\omega_1+\omega_2=\omega_3+\omega_4$ and $\vec{k}_1+\vec{k}_2=\vec{k}_3+\vec{k}_4$, which are schematically shown in (a) and (b), respectively.

$\omega_1+\omega_2=\omega_3+\omega_4$ and $\vec{k}_1+\vec{k}_2=\vec{k}_3+\vec{k}_4$. The contributions of $\hat{S}_q$ in (4) are responsible for the interference of the beams and grating formation, while the second terms $\propto\Delta\chi_q$ represent a *renormalization* of the linear optical constants due to the intensities of the beams, and are therefore responsible for phase modulations.

The system of coupled nonlinear equations (4) can sustain solutions in which one, two, or four waves are involved. All of them are of some importance in the forthcoming discussion and, accordingly, we summarize their characteristics. If only one plane wave E_1 is present in (4) with $E_2=E_3=E_4=0$ then, the solution is a plane wave with constant amplitude but an intensity-dependent phase $E_1=|E_1|\exp(i\phi)$ with $\phi\propto I_1$. This is self-phase modulation and can produce self-focusing if the beam is not a plane wave but rather a beam with an intensity profile perpendicular to $\vec{k}$, for example, a Gaussian beam. If two beams E_1 and E_2 are different from zero and $E_3=E_4=0$, then (4) can bear a direct interaction between them without generating further waves. Direct two-photon interactions are impossible in materials with $\chi^{(2)}$ only, where a third (idler) wave must be present. The system of equations (4) reduce, in this case, to two coupled nonlinear equations with $\hat{S}_1=\hat{S}_2=0$ but $\Delta\chi_1(I_1,I_2)$ and $\Delta\chi_2(I_1,I_2)\neq 0$. The two waves phase modulate each other. Finally, three waves cannot be the solution of (4) without generating an additional fourth one, and the four-wave process is the most general of all sustained by $\chi^{(3)}$ in (4). In Sec. III we will be interested in the self-modulation of a single beam and in the four-wave process in which $|E_1|\gg|E_2|$, $|E_3|$ and $|E_4|$, being the fields $E_{2,3,4}$ components generated by noise. In Sec. IV, we shall deal with the two-beam interaction forming a grating and the four-wave process rendering the diffraction of a weak probe by the grating. Further details are given in the corresponding sections.

III. STIMULATED ORIENTATIONAL SCATTERING

As mentioned in the introduction, the basic experiment for the detection of SOS consists of monitoring a cross-polarized beam with respect to the pump which, in turn, is

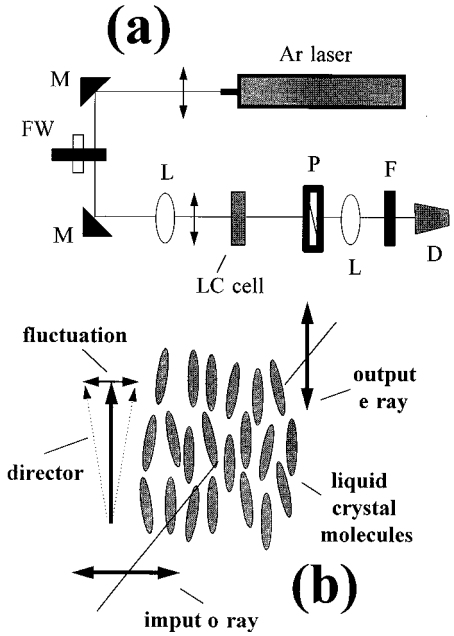

FIG. 2. (a) Basic experimental setup for the observation of SOS. A linearly polarized Ar^+ laser is sent through a planar LC cell as an *o* or *e* ray. The beam is directed by dielectric mirrors *M*. The intensity of the input beam is controlled by a filter well *FW* and focus with an input lens *L* onto the cell. The output is polarized through *P*, attenuated with neutral density filters *F*, and focused by the collecting lens *L* onto the detector *D*. In (b) we show the microscopic origin of the cross polarized SOS. The dynamic fluctuations of the director (shown schematically on the left) produce scattering from the *o* to the *e* ray and these new waves couple again to the *o* ray by means of the nonlinearity of the medium. The process may result in a stimulated wave at crossed polarization if the intensity of the input beam is high enough. See Sec. III for further details.

polarized as either an *o* or *e* ray. The schematic experimental setup is given in Fig. 2(a). A linearly polarized Ar^+ laser beam is sent through a nematic liquid crystal (LC) cell with planar alignment [1]. The cell can be rotated so that the input beam is either an *o* or an *e* ray. The transmitted signal is normally detected in crossed polarization but, as we shall show in this section, the parallel detection is also interesting and shows the consequences of saturation of the pump beam. Figure 2(b) displays the basic microscopic mechanism for SOS. In this particular case, an input *o* ray is sent through a planar nematic LC cell. The molecules, however, fluctuate around their equilibrium positions and this leads to scattering by director fluctuations [8] around its average $\langle\vec{n}\rangle$. This is shown schematically in Fig. 2(b). If we call $\hat{\vec{z}}$ the direction of $\langle\vec{n}\rangle$, $\hat{\vec{x}}$ the direction of propagation and $\hat{\vec{y}}$ the direction of the input *o* ray, the polarizability tensor for a perfectly ordered LC cell without fluctuations is

$$\begin{pmatrix} \chi_\perp & 0 & 0 \\ 0 & \chi_\perp & 0 \\ 0 & 0 & \chi_\parallel \end{pmatrix}, \tag{5}$$

where $\chi_\perp$ and $\chi_\parallel$ are the polarizabilities for the *o* and *e* rays, respectively, which are related to the microscopic polarizabilities of the individual molecules [20]. If the director fluctuates by a small angle Θ around $\langle\vec{n}\rangle$ in the direction parallel to the input polarization [as shown in Fig. 2(b)] the polarizability tensor (5) has to be rotated by the same amount and its contribution to P for $E=(0,E_y,0)$ becomes

$$P\sim\chi_\perp E_y\hat{\vec{y}}\cos^2\Theta+(\chi_\parallel-\chi_\perp)E_y\hat{\vec{z}}\sin\Theta\cos\Theta \qquad (6)$$

where $\Theta\ll 1$ is approximately given by $\sim\delta n_y/|\vec{n}|$ (δn_y is the fluctuation in the director $\perp$ to $\vec{n}$). Using the standard Ericksen-Leslie approach [21–24] for the dynamics of the director, δn_y is governed by a differential equation accounting for the total balance of torques acting on $\vec{n}$ and reads [1]

$$\gamma\frac{\partial\delta n_y}{\partial t}-K\frac{\partial^2\delta n_y}{\partial x^2}=\frac{\Delta\epsilon}{16\pi}(E_zE_y^*+E_x^*E_y), \qquad (7)$$

with γ and K the viscosity and effective elastic constants, respectively, and $\Delta\epsilon=$ dielectric anisotropy of the LC. In the steady state and assuming $\delta n_y=|\delta n_y|\exp(i\vec{k}\cdot\vec{r})$ we obtain from (7) $|\delta n_y|\propto\mathrm{Re}[E_zE_y]$. By replacing this result back into (6) with $\cos\Theta\sim 1$ and $\sin\Theta\sim\Theta\sim|\delta n_y|\propto E_zE_y$ we obtain a $\hat{\vec{z}}$ component of $P\propto E_zE_y^2$, i.e., a third-order nonlinear optical interaction along the cross-polarized direction. Using this formalism, Khoo, Liang, and Li [13] have predicted that a stimulated cross polarized wave should appear of the form $E_z\sim|E_z|\exp(igI_y)$, with $I_y\propto|E_y|^2$ and g a gain coefficient [21]. The scattering process $e\rightarrow o$ is expected to be equivalent to the $o\rightarrow e$ and bestows the same gain coefficient. This solution is approximate in the sense that for high intensities $I_y\propto|E_y|^2$, E_z may grow exponentially and render a wave of the same order of magnitude of E_y which has to wane, accordingly, if energy is to be conserved. Indeed, once we endorsed the fact that a third-order nonlinear interaction is responsible for the coupling of waves of the same energy but different polarizations, the most general process of this kind can be set forth by means of the coupled wave equations (4). For a given energy ω, there are four waves which can be coupled elastically, to wit: two *o* rays with wave vectors $\vec{k}_o=\pm n_o\vec{k}$, and two *e* rays with $\vec{k}_e=\pm n_e\vec{k}$, where $\vec{k}$ is the wave vector of the light in vacuum and $n_{e,o}$ the corresponding indices of refraction for *e* and *o* rays. In terms of the diagram in Fig. 1, these events are characterized by the degenerate four-wave mixing process $\omega_1=\omega_2=\omega_3=\omega_4=\omega$, and $\vec{k}_1=-\vec{k}_2=n_o\vec{k}$, $\vec{k}_3=-\vec{k}_4=n_e\vec{k}$. The interaction is automatically phase matched and energy conserving. Let us show briefly the consequences of (4) in the following situation: we assume a polarized input *e* ray starting at $x=0$ and the other three waves are selected at random to simulate the effect of the noise by director fluctuations. The amplitudes of the noise waves are negligible with respect to the pump. Given these initial conditions, we then study the propagation of the four waves in a typical LC cell. We employ the slowly varying envelope approximation [16–18] (SVEA) to solve the nonlinear coupled wave problem (4) and display the result in Fig. 3. We assume the fields to be plane waves for simplicity. We study the propagation through a LC cell with typical

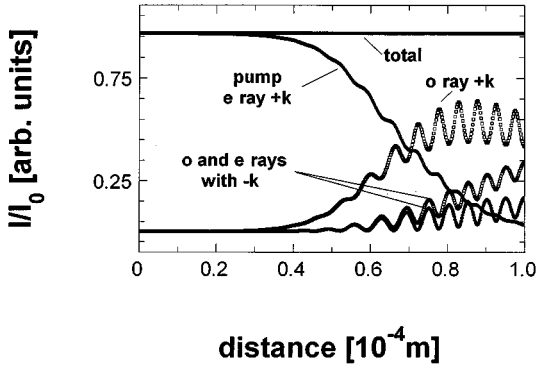

FIG. 3. Coupled waves crossing an LC cell. We use the typical parameters: $d=$thickness of the cell$=100$ μm, $n_e=1.75$, $n_o=1.55$ ($\Delta n=0.2$), $\chi^{(3)}=5\times10^{-23}$ Cm V^{-3}, incident field (*e* ray) $E_e(+\vec{\mathbf{k}})=8.7\times10^4$ V/m, energy and wave vector of the input wave $\omega=3.7\times10^{15}$ sec^{-1}, $\vec{k}=1.22\times10^7$ m^{-1} (corresponding to the 514.5 nm line of the Ar^+ laser). The *o* ray with $+\vec{k}$ and both *o* and *e* rays with $-\vec{k}$ are generated by noise at $x=0$ and taken to be fields with random phases and amplitudes $\sim$ 1% of the input wave. As the waves propagate through the cell, there is an amplification of the noise which can tone down the pump wave. The nonlinear coupled waves (4) are solved by means of the slowly varying envelope approximation. Note that the total energy remains constant but there is an effective transfer of energy between the *e* and *o* rays in the waves with $+\vec{k}$. See text for further details.

parameters given in the figure. As a function of the propagating distance x, we plot in Fig. 3 the normalized intensities of the four waves participating in the process. At $x=0$ (the input face of the cell) the *e* ray is the dominant one and the other three waves (which model the effect of noise through elastic scattering) are negligible. As the waves evolve inside the cell, the small amplitudes of the noise-induced rays start to grow out of their interactions among themselves and the pump. If the input electric field is high enough (this is the case in Fig. 3), the noise-induced waves may grow drastically to the extent that they can appreciably use up the energy of the pump beam. Note that the total energy in Fig. 3 of the four waves remains constant as required by energy conservation. On account of the interaction among the waves, the energy carried in the $+\vec{k}$ direction is larger for the *o* ray than for the *e* ray at the end face of the cell, i.e., *there has been an effective transfer of energy between the two polarizations for the waves traveling in the* $+\vec{k}$ *direction.* This is seen experimentally, as we shall show in the next subsection, by measuring both the *o*- and *e*-transmitted intensities.

Experiment

We use the liquid crystal E_7 (Ref. [25]) in a planar aligned LC cell at room temperature for the experiments. E_7 is a nematogen mixture of 4-alkyl-4′-cyanobiphenyls and terphenyls [1] with wide nematic range, a reasonably high nematic-to-isotropic phase transition temperature ($T_{N-I}\sim 63°$), and negligible residual absorption at the 514.5 nm line of the Ar^+ laser (less than 0.01 cm^{-1}). The negligible absorption and high T_{N-I} prevent a possible jump to

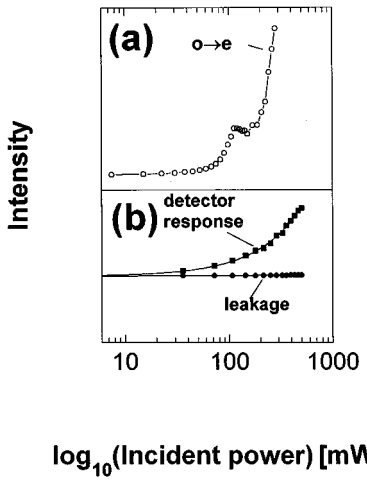

FIG. 4. (a) Crossed polarized scattering $o \rightarrow e$ for the liquid crystal E_7 at room temperature as a function of input intensity. Note the presence of a sudden increase followed by a plateau and a second sharp increase. The plateau is associated with the power at which the pump beam starts to be depleted, as we shall show in Fig. 5. In (b) we show the response of the detector to a diffuser placed at the cell position and, in addition, the leakage observed through an empty cell. The response is linear (note the logarithmic horizontal scale) and the leakage negligible within the experimental error.

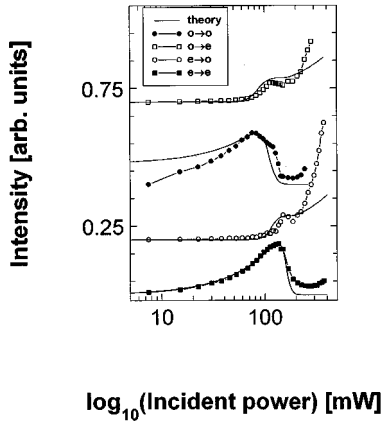

FIG. 5. The four possible scattering configurations $o \rightarrow e$, $o \rightarrow o$, $e \rightarrow o$, and $e \rightarrow e$ in the planar oriented liquid crystal E_7. The cross polarized signals, as in Fig. 4(a), show a flat region followed by an increase at a certain threshold, a plateau, and a further increase at higher powers. The parallel polarized signals, on the contrary, increase almost linearly with the input pump up to a point (coincident with the increase of the cross polarized scattering) where the signal starts to decrease. These features reveal the saturation of the pump by the cross-polarized wave as in Fig. 3. The solid lines are theoretical curves with typical parameters for E_7 using the degenerate four-wave mixing approach explained in the text.

the isotropic phase by residual heating or related effects. The alignment is achieved by the Chatelain method [26] of rubbing the cell windows along a fixed direction with 0.3 μm grain size diamond paste. A 100 μm mica spacer is used between the two scraped windows to form the cell. The planar alignment is checked by the conoscopic patterns in transmission through crossed polarizers under the microscope [2]. The cell is mounted at the focal point of the first lens in Fig. 2(a) in a rotating frame which allows a change from e to o rays with minimum effort. Figure 4(a) shows a typical cross-polarized spectrum of SOS from the o to the e ray as a function of input power. A sudden increase in the intensity is found above a certain threshold and this is followed by a plateau and a second sharp increase. This is telling us that the cross-polarized stimulated scattering is a more complicated process than a simple exponential growth. To test the performance of the setup in Fig. 2(a), and check that none of these features are artificial, we show in Fig. 4(b) the result of replacing the LC cell with a diffuser and an empty cell, respectively. The diffuser produces a fairly isotropic distribution of polarizations and the signal is proportional to the input power. The empty cell is observed in crossed polarization and gives a measure of possible background signals and leakage. The detector response is linear and the leakage negligible within the experimental error.

Figure 5 exhausts all possible combinations of input-output polarizations. The input wave is either an e or o ray and the analysis is done for parallel or crossed polarization to bring forth the four possible cases $e \rightarrow e$, $e \rightarrow o$, $o \rightarrow e$ and $o \rightarrow o$. As explained before, no essential difference is expected between the cases $e \rightarrow o$, $o \rightarrow e$ and the same holds for $e \rightarrow e$, $o \rightarrow o$. Figure 5 shows that the cross polarized cases are delineated by a flat region (of the same order of magnitude of a leakage signal) followed by a sudden increase, a plateau, and a second increase at higher input powers. Conversely, the parallel polarized cases show a constant linear increase with the input power up to a point (coincident with the increase of the corresponding cross-polarized signal) in which the signal starts to fade away. *By increasing the input power above this point we obtain less light polarized in the same direction of the laser after transmission.* There is a small difference between the thresholds for SOS when starting with an e or o ray, as seen in Fig. 5. This disparity is, however, attributed to small differences in the focal area when the cell is rotated and not to a fundamental physical phenomenon. Note that the experimental results are given as a function of input power. In order to transform the incident power to an input electric field, the focal area (beam waist) has to be known accurately. This is a source of uncertainty on which we shall comment later. If we replace the LC cell in Fig. 2(a) with an identical cell filled with E_7 in the nematic state but unoriented (unpolished windows), we obtain the result displayed in Fig. 6 for the same input power range. The result in Fig. 6 attests that a liquid crystal in the nematic state without orientation imposed by the boundaries is a very effective *diffuser* and none of the features observed in the aligned sample in Fig. 5 are seen here. A possible source of problems in the experiment is the presence of transverse phase modulation of the input beam [27] which may change the far field beam profile and the amount of light gathered by the collecting lens in Fig. 2(a). The collecting lens and detector have a fixed numerical aperture and the amount of light detected will vary if the beam is divergent or has any other variation in the far field as a function of the intensity. The signal will not vary, however, if the main contribution comes from parallel paraxial rays. In order to check this, we measure the SOS signal for different distances be-

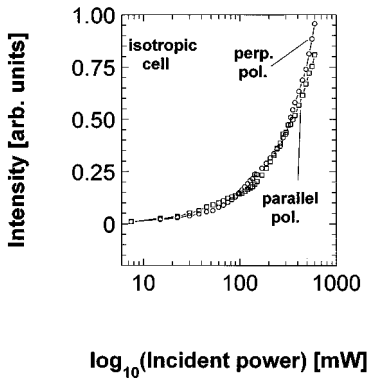

FIG. 6. Transmitted intensity for parallel and crossed polarizations when the planar aligned LC cell in Fig. 2(a) is replaced by an identical cell with no orientation imposed on the nematic. Both signals increase linearly (note the logarithmic scale) with the input power and are the same within the experimental error. This plot shows not only the effectiveness as a diffuser of a nematic (based on the elastic scattering mechanism explained in the text) but also that none of the features of Fig. 5 appear in an unoriented sample.

tween the cell and the collecting lens. This is shown in Fig. 7 where we use a fixed collecting lens of 10 cm focal length and 5 cm diameter and measure the cross-polarized scattering for different distances between the cell and the lens. It is quite clear that the features of the signal (in particular, the plateau) come from parallel paraxial rays and not from variations in the light collected by the fixed numerical aperture of the detection stage.

The depletion of the pump wave and the existence of a plateau in the cross-polarized signals can be well accounted for by the theoretical curves obtained from the four-wave mixing formalism presented above and are shown in Fig. 5.

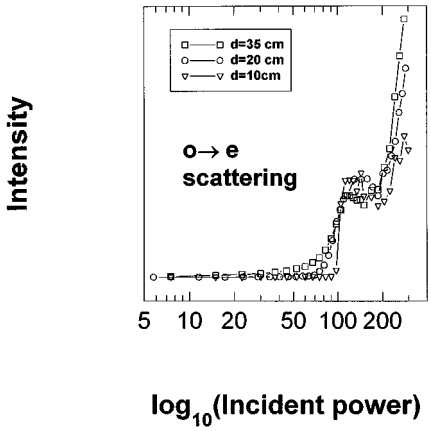

FIG. 7. A nonlinear film like an LC cell with an oriented nematic can produce wave-front distortions in a beam and therefore change the amount of light collected in the far transmitted field by a detector with a fixed numerical aperture. No change is expected if the main contribution to the signal comes from parallel paraxial rays crossing the sample. Here we show three cross-polarized SOS signals obtained by changing the distance d between the collecting lens ($f=10$ cm) and the LC cell. All curves show the same features at the same input powers, in particular, the plateau describing the saturation of the pump is clearly reproduced in all of them.

The solid lines in Fig. 5 have been calculated assuming noise of negligible random amplitude ($\ll 1\%$ of the input power) and arbitrary phases, being coupled to the incoming wave. Using a sufficiently large set of initial conditions (10^4 in this case) by means of random numbers and solving (4) in the SVEA approximation for each of them, we obtain the average power being transmitted through the cell by the different waves. The calculation is performed with typical parameters for E_7 from the literature [1] and the cell thickness imposed in our experiment of $d=100$ μm. There are two adjustable parameters in each theoretical curve shown in Fig. 5. The first one is trivial and simply scales the vertical axis to adjust the curves to the arbitrary units of the experiment. The second one scales the horizontal axis and has a physical origin. If we knew the exact area (A) of the waist at the focal point of the first lens in Fig. 2(a) we could transform the intensity (I) into an incident electric field through $E^2=I/c\epsilon_0 A$. We estimate the spot diameter of the laser on the sample to be of the order of 0.1 mm, but a factor of 2 error in this value (which leads to a factor of 4 in the area) could be easily admitted. It is better to use an adjustable parameter to scale the horizontal axis of the calculations in Fig. 5 to obtain closest agreement with the experiment. Although the cross-polarized signals in Fig. 5 seem to increase faster than the calculations after the plateau, the general agreement between theory and experiment is regarded as excellent. In particular, the decrease in the parallel polarized signals and the simultaneous presence of a plateau in the crossed ones is correctly predicted. Further improvement in the comparison with the experiment can be achieved by introducing phenomenological losses in the nonlinear system of equations (4).

It is probably worth noting at this stage that the generation and coupling of noise with the pump is a coherent process, but two independent fluctuations occurring at different times are of course incoherent with respect to each other. The total transmitted intensity in the theoretical curves of Fig. 5 is therefore calculated as an incoherent sum of the different initial conditions imposed by the noise, due to the fact that the signal is integrated over a long ($\sim$ 10 sec) interval. The characteristic time for fluctuations, [8,9] however, is fixed by the director dynamics and is typically in the millisecond range. This is very long in comparison with the time it takes the light to travel to an external mirror and come back to the cell for typical laboratory dimensions. In this manner, one can take the cross-polarized beam generated by noise and amplified coherently with the pump by SOS, rotate it, reflect it on a mirror, and mix it again with the input beam inside the cell. The beam will be coherent with respect to the pump under these circumstances and this is the method for observing phase conjugation [13] using SOS. It is normally called *self-starting phase conjugation* because the noise triggers the process.

IV. FOUR-WAVE MIXING AS A PHOTONIC CRYSTAL PROBLEM

We now turn to a different aspect of $\chi^{(3)}$ nonlinearities. The aim of this section is to show the equivalence between the four-wave mixing equations (4) and the problem of calculating the electromagnetic bands in a multilayer or, in other words, in a one-dimensional (1D) photonic

crystal [15]. Toward this end, let us assume $|E_2|=|E_4|=|E_{\text{pump}}|\gg|E_1|, |E_3|$ in (4), i.e., the amplitudes of two of the beams are much larger than the other two, and will be called *pump beams*. The fields E_1 and E_3 will be called probe and diffracted beams, respectively. We assume $\omega_2=\omega_4=\omega_{\text{pump}}$ and $\omega_1=\omega_3=\omega$. The wave vectors of the pump beams form an angle $\beta=\vec{k}_2\cdot\vec{k}_4/|\vec{k}_2||\vec{k}_4|$ between them. It is also considered that any change in the intensities of the pump beams is so small, that they are to be considered constant for computational purposes; in other words, there is negligible *amplification* or *depletion* of the beams, in contrast to the preceding section. Under these circumstances we can approximately decouple the four equations (4) into two pairs, one for the pump beams and one for the probe and diffracted beams. The equations for the pumps read

$$\left(\nabla^2+\frac{n^2\omega_{\text{pump}}^2}{c^2}\right)E_2=3\mu_0\omega_{\text{pump}}^2\chi^{(3)}E_2[|E_2|^2+2|E_4|^2] \tag{8}$$

and

$$\left(\nabla^2+\frac{n^2\omega_{\text{pump}}^2}{c^2}\right)E_4=3\mu_0\omega_{\text{pump}}^2\chi^{(3)}E_4[|E_4|^2+2|E_2|^2]. \tag{9}$$

Thence, there are no *interference* terms $\hat{S}_{2,4}$ which are of order $\sim|E_{\text{probe}}|^2$ but both beams phase modulate each other. This is the two-beam interaction through $\chi^{(3)}$ mentioned in Sec. II. Since both beams have the same modulus $|E_{\text{pump}}|$ the amount of modulation is the same for both. The two equations (8) and (9) can be rewritten as

$$\left(\nabla^2+\frac{\tilde{n}^2\omega_{\text{pump}}^2}{c^2}\right)E_q=0,\quad q=2,4 \tag{10}$$

where $\tilde{n}^2=n^2-9\mu_0\omega_{\text{pump}}^2\chi^{(3)}c^2|E_{\text{pump}}|^2$ is the *renormalized* index of refraction due to $\chi^{(3)}$. Equation (10) implies that the interference pattern between E_2 and E_4 is slightly changed by the presence of $\chi^{(3)}$ because the effective wave vector for propagation is changed from $n\vec{k}$ to $\tilde{n}\vec{k}$. This effect is nevertheless small and we can ignore it for the pumps. We therefore consider the interference pattern of the two pumps as if they were a linear medium. We assume the two beams to be polarized along the same direction. The two pumps will produce an intensity pattern of the form

$$\begin{aligned} I_{\text{pump}}&\propto(E_2+E_4)(E_2+E_4)^* \\ &=2|E_{\text{pump}}|^2[1+\cos((\vec{k}_2-\vec{k}_4)\vec{r})], \end{aligned} \tag{11}$$

which comprises a constant term and an interference grating $\propto\cos[(\vec{k}_2-\vec{k}_4)\vec{r}]$. The grating has planes of constant phase perpendicular to $(\vec{k}_2-\vec{k}_4)$.

We now obtain the other two decoupled equations for the probe E_1 and the diffracted E_3 beams. We assume both fields $E_{1,3}$ for the time being to be polarized in the same direction of $E_{2,4}$. The interesting part of the physics for these beams comes from the interference terms $\hat{S}_{1,3}$ which are now $\neq0$ and of order $|E_{\text{pump}}|^2$. There is a renormalization of the index of refraction coming from the terms $\propto\Delta\chi_{1,3}$ and the constant part of the interference grating in (11). Notwithstanding, this renormalization is the same for both beams as in (10), and we absorb it in an effective index $\tilde{n}$. The equations read

$$\left(\nabla^2+\frac{\tilde{n}^2\omega^2}{c^2}\right)E_1=\omega^2\zeta\cos[(\vec{k}_2-\vec{k}_4)\vec{r}]E_3, \tag{12}$$

and

$$\left(\nabla^2+\frac{\tilde{n}^2\omega^2}{c^2}\right)E_3=\omega^2\zeta\cos[(\vec{k}_2-\vec{k}_4)\vec{r}]E_1, \tag{13}$$

with $\zeta=6\mu_0\chi^{(3)}|E_{\text{pump}}|^2$. This is the essence of the four-wave mixing problem as carried out in the majority of cases, with a weak probe with respect to the pump reducing the problem of four nonlinear differential equations (4) to two *linear* coupled differential equations for the probe and diffracted beams (12) and (13). We now define the trivial combinations $E^+=E_1+E_3$ and $E^-=E_1-E_3$ which, according to (12) and (13) will satisfy

$$\left(\nabla^2+\frac{n^2\omega^2}{c^2}\right)E^\pm=\pm\omega^2\zeta\cos[(\vec{k}_2-\vec{k}_4)\vec{r}]E^\pm. \tag{14}$$

Both equations (14) contain the same information, as we shall show later, and therefore it suffices to consider only one. Equation (14) for E^+ can be written as

$$\left(\nabla^2+\frac{\epsilon(\vec{r})\omega^2}{c^2}\right)E^+=0, \tag{15}$$

where $\epsilon(\vec{r})=\tilde{n}^2-c^2\zeta\cos[(\vec{k}_2-\vec{k}_4)\vec{r}]$ is a *position-dependent dielectic function* representing the 1D periodic modulation with wave vector $\vec{k}_2-\vec{k}_4$ induced by the pump beams. The reader will recognize immediately (15) as the Maxwell equation for the electric field of the light in a dielectric layered system which has, in this case, a modulation proportional to $\epsilon(\vec{r})\propto\cos[(\vec{k}_2-\vec{k}_4)\vec{r}]$. The equation for E^- is equal to (15) but with $\epsilon(\vec{r})=\tilde{n}^2+c^2\zeta\cos[(\vec{k}_2-\vec{k}_4)\vec{r}]$, which is the same grating but displaced by a constant phase $\phi=\pm\pi$. Note that the description of both the probe and diffracted beams hinges on the problem of finding the bands in a grating for only *one* field E^+. The reason for this will soon be clear.

As in any standard band structure in a 1D layered system, two cases can be easily distinguished: off- and on-axis propagation with respect to the axis of the grating along z $[z\|(\vec{k}_2-\vec{k}_4)]$. We consider first on-axis propagation for simplicity. The meaning of this in terms of the phase-matching condition shown in Fig. 1 is given in Fig. 8. Equation (15) is solved by expanding the field into a Fourier series of the form

$$E(z)=\sum_G A(G)e^{i(k_z+G)z}, \tag{16}$$

with $G=0,\ \pm|\vec{k}_2-\vec{k}_4|,\ \pm2|\vec{k}_2-\vec{k}_4|,\ldots,$ etc. The photonic band structure along the axis of the grating is therefore transformed into the eigenvalue problem [14]

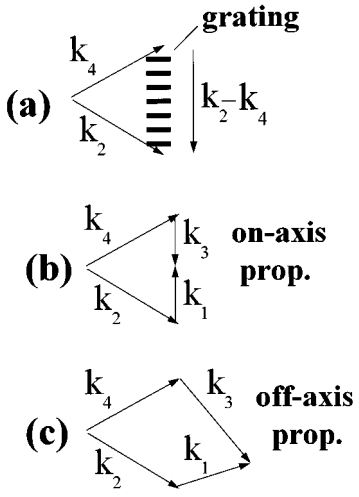

FIG. 8. (a) Pump beams forming a grating along $\vec{k}_2-\vec{k}_4$. The beams are assumed to be copolarized perpendicular to the plane of the page. (b) On-axis propagation. Both the probe $\vec{k}_1$ and diffracted $\vec{k}_3$ beams are along $\vec{k}_2-\vec{k}_4$, and satisfy the phase matching condition of Fig. 1(b). Both polarizations, $\parallel$ and $\perp$ to the plane of the page, breed the same bands in this case. (c) Off-axis propagation. This case produces two different types of bands according to the polarization of the probe and diffracted beams with respect to the pumps. See text for further details.

$$\sum_{G'} \hat{\kappa}(G-G')(k_z+G')^2 A(G') = \frac{\omega^2}{c^2} A(G), \qquad (17)$$

where $\hat{\kappa}(G-G')$ is the Fourier transform of the inverse of the position-dependent dielectric function

$$\hat{\kappa}(G) = \frac{1}{a}\int_a dz e^{iGz} \frac{1}{\epsilon(z)}, \qquad (18)$$

with $a = 2\pi/|\vec{k}_2-\vec{k}_4|$.

Consider a typical example of grating formation through $\chi^{(3)}$ in a liquid crystal. As explained in the introduction, several mechanism can contribute to $\chi^{(3)}$. Let us consider for simplicity those situations in which $\chi^{(3)}$ comes mainly from molecular reorientations. This is a case that has been extensively studied in the literature [21,28–30] and therefore we do not repeat its derivation. The important point for our purposes is that the reorientation can form a grating with typical parameters in the range $c^2\zeta \sim 10^{-1}$–10^{-3}, while $\tilde{n}^2 \sim 2.2$–2.5. Accordingly, we expand

$$\frac{1}{\epsilon(z)} \sim \frac{1}{\tilde{n}^2} + \frac{2c^2\zeta}{\tilde{n}^4}(e^{i|\vec{k}_2-\vec{k}_4|z} + e^{-i|\vec{k}_2-\vec{k}_4|z}), \qquad (19)$$

and obtain for $\hat{\kappa}(G)$ in (18)

$$\hat{\kappa}(G) = \frac{\delta_{G,0}}{\tilde{n}^2} + \frac{2c^2\zeta}{\tilde{n}^4}[\delta_{G,-|\vec{k}_2-\vec{k}_4|} + \delta_{G,+|\vec{k}_2-\vec{k}_4|}]. \qquad (20)$$

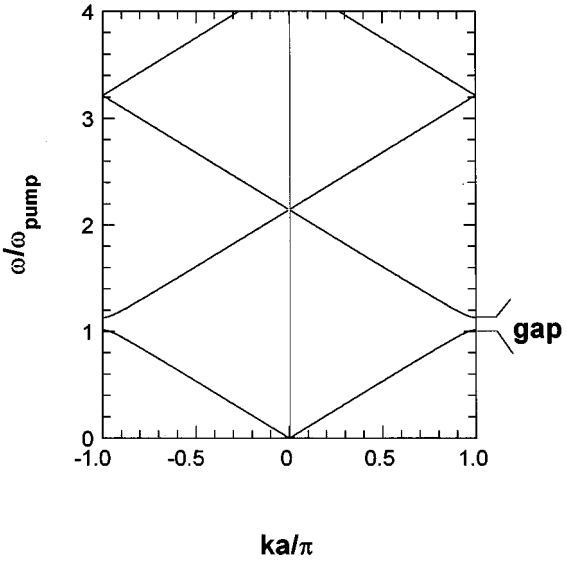

FIG. 9. Photonic bands for on-axis propagation in the grating formed by two interfering copolarized Ar^+-laser beams. We used 51-plane waves in (17) to solve the eigenvalue problem. Convergence is achieved very easily due to the particular form of the perturbed dielectric function (20). Wave vectors are normalized by $a/\pi = 2/|\vec{k}_2-\vec{k}_4|$ and energies by the incident pump frequency. Note the existence of a gap for energies slightly above ω_{pump}. The problem is equivalent to the one of electrons in a weak periodic potential and the wave vectors in each band are well approximated by (22).

By substituting (20) into (17) (which is the equivalent of the *nearly free electron model in a weak periodic potential* but for electromagnetic waves) the band structure for on-axis propagation can be solved.

In Fig. 9 we show a band structure for propagation along the axis of the grating for typical parameters of a liquid crystal. We take $\tilde{n}^2 = 2.25$, and $c^2\zeta = 10^{-1}$ and use a basis of 51 planewaves in (17) to solve the bands. A relatively small number of plane waves are needed to achieve convergence in (17) due to the special form of $\hat{\kappa}(G)$ which contains only one Fourier coefficient $\neq 0$. This is in contrast to normal photonic band structure calculations where the sharp dielectric interfaces require a basis of $\sim 200-500$ plane waves [15]. The grating is taken to be formed by two copolarized Ar^+ laser beams ($\lambda = 514.5$ nm) at 45° producing a lattice with $G = |\vec{k}_2-\vec{k}_4| \sim 4\times 10^7\ \text{m}^{-1}$. The full four-wave mixing problem described by the nonlinear differential equations (4) has therefore been transformed into a trivial example of bands in solid-state physics. Since the perturbation in refractive index (20) is small and has only *one* Fourier component G, only one gap in first order at the edge of the Brillouin zone in the first band is opened. The other crossings of the bands at $\vec{k}=0$ or $k_z = \pm G/2$ have only small splittings from second or higher order perturbations. The bands can be labeled by a principal number n and the leading term of the eigenvectors according to perturbation theory will be

$$E \sim e^{i(\pm k_z \mp nG)z}. \qquad (21)$$

Except at the Bragg plane in the gap, where degenerate per-

turbation theory has to be applied, the eigenvectors will be well described by a perturbation series on (21). For the lowest band along k_z, for example,

$$E \sim c_0 e^{ik_z z} + c_1 e^{i(k_z - G)z} + c_2 e^{i(k_z - 2G)z} + \cdots, \qquad (22)$$

where $c_0 \sim O(1)$ and $c_{1,2} \ll c_0$ of order $c_1 \sim |\chi^{(3)}||E_{pump}|^2/G$, $c_2 \sim |\chi^{(3)}|^2|E_{pump}|^4/G^2, \ldots$, etc.

The reason why we reduced the probe and diffracted beams to a single field E^+ moving in periodic dielectric is now clearer from (22). E^+ contains all the information in itself. Since plane waves are not exact eigenvectors of the problem, each selected point in the band structure is necessarily a linear combination of plane waves like (22). The first term in (22) represents the probe with $\vec{k}_1 = k_z$ while the diffracted beam is given by the second leading term in the perturbation with $\vec{k}_3 = k_z - G$. Note that this satisfies automatically the phase-matching condition [see Fig. 8(b)]. The third and higher order terms in (22) are nothing but *umklapp processes* [31] as known from electronic bands and appear naturally in this formalism as a trivial consequence of the expansion (22). The ratios $|c_1|^2/|c_0|^2$, $|c_2|^2/|c_0|^2, \ldots$, etc., give automatically the diffraction efficiencies for each process. Note that this information is condensed in a single calculation for any arbitrary probe energy with respect to the pump.

In addition, off-axis propagation contains further information on the diffraction efficiencies for different polarizations. It is well known [15] from the calculation of band structures for electromagnetic waves that off-axis propagation in a 1D grating implies a breaking of symmetry. If the axis of the grating is along $\hat{z}$ and the planes of constant phase in $\cos[(\vec{k}_2 - \vec{k}_4)\vec{r}]$ are along the $\hat{x}$-$\hat{y}$ plane, both polarizations $\hat{x}$ and $\hat{y}$ render the same bands for on-axis propagation. Conversely, off-axis propagation, for example $\vec{k}$ in the $(\hat{x}-\hat{z})$ plane, distinguishes between $\hat{y}$ and $(\hat{x}-\hat{z})$ polarized waves [15] and each band contains the information on the different diffraction efficiencies as in (22) for the different polarizations, resulting in a massive simplification of the information needed for different four-wave mixing processes.

Finally, note that the gap in Fig. 9 predicts no possible four-wave mixing effect for on-axis propagation and energies slightly above that of the laser forming the grating. The position of this gap can be changed by small amounts by changing the interference angle β between the input beams, but will always exist around ω_{pump}. Although of very limited use, the sample behaves formally as a dielectric mirror for strict on-axis propagation at these energies. There will be an evanescent mode at the surface producing 100% refectivity of the probe beam but no propagation. This gap is not absolute and actually does not exist for off-axis propagation, as known from the theory of dielectric multilayers [15]. The largest efficiency for the on-axis four-wave mixing process, given by $|c_1|^2/|c_0|^2$, will be for ω slightly below or above the gap, where the eigenvector is a linear combination of the form

$$E \sim c_0(e^{ik_z z} \pm e^{i(k_z - G)z}), \qquad (23)$$

as known from standard band theory.

V. CONCLUSIONS

Several effects related to the presence of a large third-order nonlinear optical susceptibility $\chi^{(3)}$ in liquid crystals have been analyzed. In Sec. III we presented experimental data on stimulated orientational scattering and its interpretation as a degenerate four-wave mixing effect producing a net transfer of energy between the *o* and *e* rays. Saturation phenomena of the pump have been discussed in addition. In Sec. IV we showed how the four-wave mixing equations and the theory of photonic band structures are intimately related. The formalism of Sec. IV clearly surpasses the application to liquid crystals. We feel, however, that it is in those materials where $\chi^{(3)}$ is large, and CW experiments can be carried out, that the formalism is most relevant. In materials where four-wave mixing phenomena have to be studied with high-energy pulsed lasers (like semiconductors) the additional complication of the time evolution of the grating exists. The latter is normally treated within the density-matrix formalism [17] and would need a time-dependent band structure calculation of debatable practical use. In Sec. IV we demonstrated through a simple example how the photonic band structure approach simultaneously contains data on the diffraction efficiencies of simple and umklapp four-wave mixing events and the polarization dependencies for all possible directions of propagation and incident energies of the probe beam, resulting in a major compression of information within a very simple calculation.

In Sec. IV the case of grating formation by copolarized beams was treated for simplicity. However, further interesting cases exist in laser-induced gratings. An example is the grating formation by cross-polarized beams which results in a continuous change from circular, to elliptical, to linearly polarized waves inside the LC cell, producing a sinusoidal distribution in terms of polarization [1]. These cases should breed interesting ground tests for the photonic crystal approach to wave mixing.

ACKNOWLEDGMENTS

Pablo Etchegoin wishes to thank the European Union for financial support at the Cavendish Laboratory in Cambridge (U.K.). This work has been supported by EPSRC (U.K.).

[1] For a general review of the field as well as a comprehensive list of references of the latest advances, see I. C. Khoo, *Liquid Crystals, Physical Properties and Nonlinear Optical Phenomena* (Wiley, New York, 1995); see also I. C. Khoo and S. T. Wu, *Optics and Nonlinear Optics of Liquid Crystals* (World Scientific, London, 1993) and references therein.

[2] The basic aspects of the properties of the director in the continuum theory of liquid crystals can be obtained from S. Chandrasekhar, *Liquid Crystals*, 2nd ed. (Cambridge University Press, Cambridge, England, 1994) and P. G. de Gennes, *The*

Physics of Liquid Crystals (Clarendon Press, Oxford, 1974).

[3] Second harmonic generation from nematics can be observed, however, under some circumstances (normally associated with distortions, external fields, surface effects, or electric-quadrupole interactions); see, Ou-Yang Zhong-Can and Xie Yu-Zhang, Phys. Rev. A **32**, 1189 (1985); M. I. Barnik, L. M. Blinov, A. M. Dorozhkin, and N. M. Shtykov, Mol. Cryst. Liq. Cryst. **98**, 1 (1983); S. M. Arakelyan, Yu. S. Chilingaryan, G. L. Grigoryan, G. A. Lyakhov, S. Ts. Nersisyan, and Yu. P. Svirko, *ibid.* **71**, 137 (1981).

[4] N. F. Pilipetski, A. V. Sukhov, N. V. Tabiryan, and B. Ya Zel'dovich, Opt. Commun. **37**, 280 (1981); I. C. Khoo, Phys. Rev. A **25**, 1636 (1982).

[5] D. V. G. L. Narasimha and D. K. Agrawal, Phys. Lett. **37A**, 383 (1971); P. Etchegoin and R. T. Phillips, Phys. Rev. E **54**, 2637 (1996).

[6] J. W. Shelton and Y. R. Shen, Phys. Rev. A **5**, 1867 (1972).

[7] I. C. Khoo, J. Y. Hou, G. L. Din, Y. L. He, and D. F. Shi, Phys. Rev A **42**, 1001 (1990); I. C. Khoo, Phys. Rev. A **23**, 2077 (1981).

[8] Grupe d'Etudes des Cristaux Liquides (Orsay), J. Chem. Phys. **51**, 816 (1969).

[9] The scattering is, strictly speaking, *quasielastic* but the energy transfer $\Delta\omega$ is in the range [8] $\sim 10^3$–10^7 $\sec^{-1}$ which is negligible compared to the laser energy in the visible range. The scattering can be considered elastic for all practical purposes here.

[10] H. Haken, *Light: Laser Light Dynamics* (North Holland, Amsterdam, 1985), Vol. II.

[11] R. Benzi, A. Sutera, and A. Vulpiani, J. Phys. A **14**, L453 (1981); A. R. Bulsara and L. Gammaitoni, Phys. Today **49**(3), 39 (1996).

[12] B. Ya Zel'dovich, S. K. Merzlinkin, N. F. Pilipetskii, and A. V. Sukhov, Pis'ma Zh. Éksp. Teor. Fiz. **41**, 418 (1985) [JETP Lett. **41**, 514 (1985)].

[13] I. C. Khoo, Yu Liang, and H. Li, Opt. Lett. **20**, 130 (1995).

[14] E. Yablonvitch, Phys. Rev. Lett. **58**, 2059 (1987); M. Plihal and A. A. Maradudin, Phys. Rev. B **44**, 8565 (1991); P. Etchegoin and R. T. Phillips, Phys. Rev. B **53**, 12 674 (1996), and references therein.

[15] J. D. Joannopoulos, R. D. Meade, and J. N. Winn, *Photonic Crystals* (Princeton Universty Press, Princeton, NJ, 1995).

[16] B. E. A. Saleh and M. C. Teich, *Fundamentals of Photonics* (Wiley, New York, 1991).

[17] A. Yariv, *Optical Electronics* (Saunders HBJ, New York, 1991); *Quantum Electronics* (Wiley, New York, 1991).

[18] Y. R. Shen, *The Principles of Nonlinear Optics* (Wiley, New York, 1984).

[19] Assuming χ and $\chi^{(3)}$ dispersionless is a good approximation far from the lowest HOMO to LUMO absorption band. This is the case for the liquid crystal of interest here, which has the lowest absorption band in the ultraviolet while the experiments are performed at the green 514.5-nm line of an Ar^+ laser.

[20] The polarizability of a group of LC molecules is not directly proportional to the polarizabilities of the individual molecules because *local field corrections* play an important role in the final result. On the problem of local fields in LC, see Ref. [1] and also L. M. Blinov, *Electro-optical and Magneto-optical Properties of Liquid Crystals* (Wiley, New York, 1983).

[21] I. C. Khoo, IEEE J. Quantum Electron. **QE-22**, 1268 (1986).

[22] W. H. de Jeu, *Physical Properties of Liquid Crystalline Materials* (Gordon and Breach, New York, 1980).

[23] E. B. Priestley, P. J. Wojtowicz, and P. Sheng, *Introduction to Liquid Crystals* (Plenum, New York, 1975).

[24] The SVEA approximation for plane waves implies that we simultaneously ignore the transverse part $\nabla_\perp^2$ of $\nabla^2=\nabla_\perp^2+\nabla_x^2$ in (4) ($\hat{x}$=direction of propagation) and assume $|\partial^2 A(x)/\partial x^2| \ll |2k\partial A(x)/\partial x|$ for fields of the form $E=A(x)\exp(\pm ikx)$.

[25] Purchased from Merck Ltd., Poole, England.

[26] P. Chatelain, Bull. Soc. Fr. Minér. **66**, 105 (1943); J. L. Lanning, Appl. Phys. Lett. **21**, 15 (1972); D. Berreman, Phys. Rev. Lett. **28**, 1683 (1972).

[27] I. C. Khoo, T. H. Liu, and P. Y. Yan, J. Opt. Soc. Am. B **4**, 115 (1987).

[28] B. Ya Zel'dovich, N. V. Tabiryan, and Yu S. Chilingaryan, Zh. Éksp. Teor. Fiz. **81**, 72 (1981) [Sov. Phys. JETP **54**, 32 (1981)].

[29] N. V. Tabiryan and B. Ya Zel'dovich, Mol. Cryst. Liq. Cryst. **62**, 237 (1980).

[30] H. L. Ong, Phys. Rev. A **28**, 2393 (1983).

[31] Umklapp processes involving $\chi^{(3)}$ are known in a different context in a third harmonic generation by cholesteric liquid crystals [6]. In this case, the periodicity imposed by the *pitch* of the liquid crystal provides the lattice wave vector $\vec{G}$ needed to complete the phase matching.